Thermoelectric Properties of Zinc-Doped $Cu_5Sn_2Se_7$ and $Cu_5Sn_2Te_7$

Cheryl Sturm,[a] Leilane R. Macario,[a] Takao Mori,[b] and Holger Kleinke*[a]

SUPPLEMENTARY INFORMATION

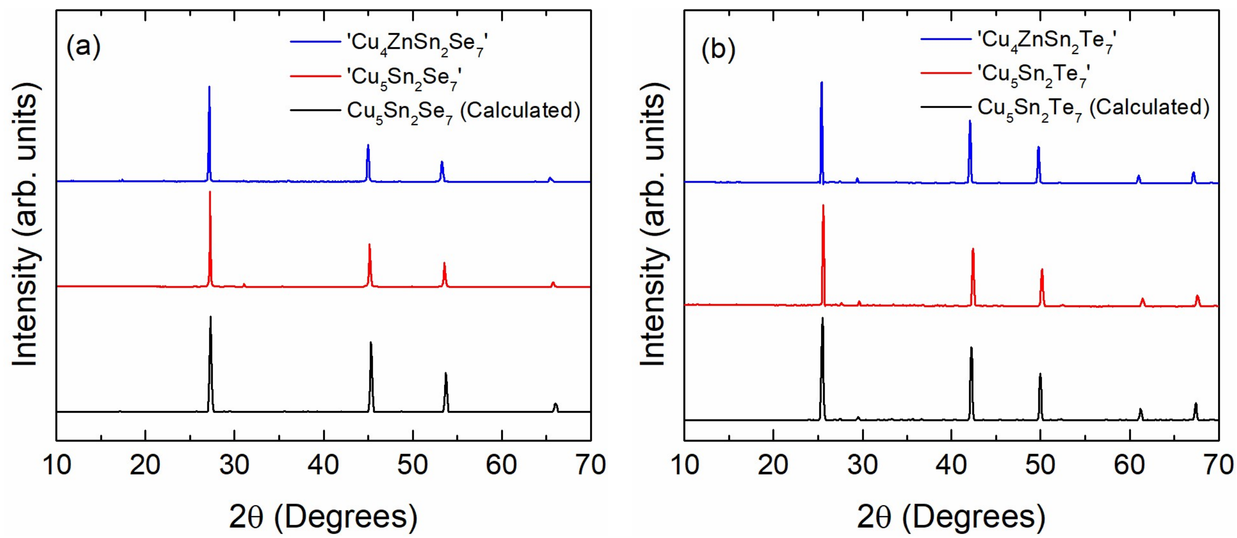

Figure S1. Calculated and experimental X-ray powder patterns of (a) '$Cu_5Sn_2Se_7$' and '$Cu_4ZnSn_2Se_7$', and (b) '$Cu_5Sn_2Te_7$' and '$Cu_4ZnSn_2Te_7$'.

Table S1. Refined lattice parameters of $Cu_{5-x}Zn_xSn_2Q_7$.

	'$Cu_5Sn_2Se_7$'	'$Cu_4ZnSn_2Se_7$'	'$Cu_5Sn_2Te_7$'	'$Cu_4ZnSn_2Te_7$'
a (Å)	12.5580(8)	12.6067(5)	13.544(1)	13.5925(2)
b (Å)	5.6570(2)	5.6771(1)	6.0442(2)	6.0696(2)
c (Å)	8.9991(5)	8.9270(6)	9.5771(3)	9.4935(2)
β (º)	98.170(5)	98.135(3)	98.063(3)	98.302(2)
V (Å^3)	632.81(7)	632.47(5)	776.26(5)	775.02(3)

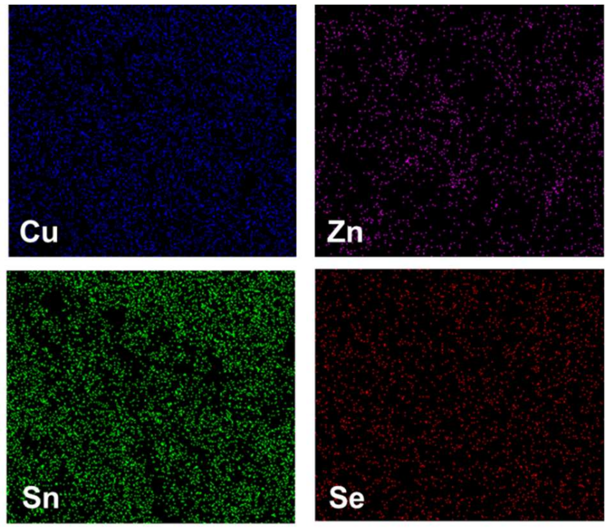

Figure S2. EDX maps of '$Cu_4ZnSn_2Se_7$'.

Table S2. Results of EDX confirming homogeneity of '$Cu_4ZnSn_2Se_7$' (STDEV = standard deviation, using eight data points).

Element	theor. at.-%	exper. at.-%	STDEV
Cu (K)	28.6	29.4	1.2
Zn (K)	7.1	6.8	1.1
Sn (L)	14.3	14.7	0.3
Se (L)	50.0	49.1	1.9

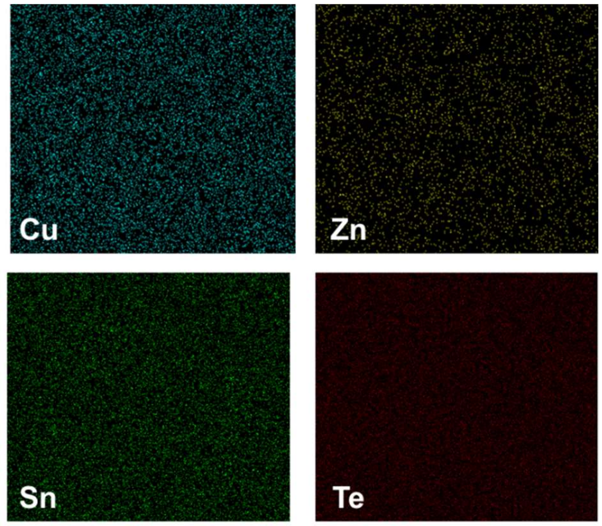

Figure S3. EDX maps of $Cu_4ZnSn_2Te_7$.

Table S3. Results of EDX confirming homogeneity of sample '$Cu_4ZnSn_2Te_7$' (STDEV = standard deviation, using eight data points).

Element	**theor. at.-%**	**exper. at.-%**	**STDEV**
Cu (K)	28.6	28.0	1.8
Zn (K)	7.1	7.3	0.8
Sn (L)	14.3	14.7	1.1
Te (L)	50.0	50.0	1.3

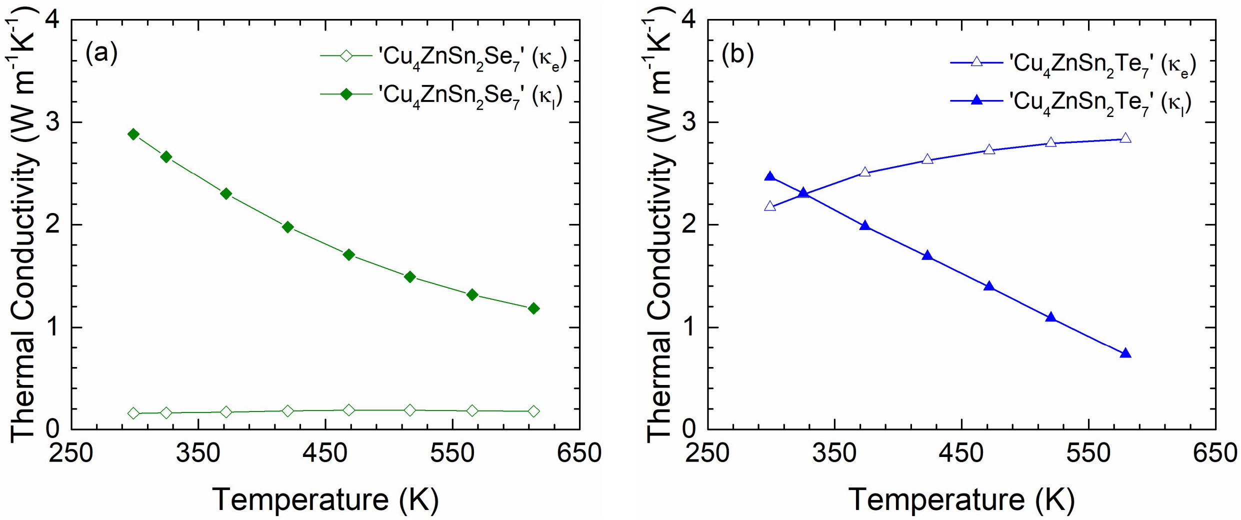

Figure S4. Temperature dependence of the electrical and lattice components of the thermal conductivity of (a) '$Cu_4ZnSn_2Se_7$' and (b) '$Cu_4ZnSn_2Te_7$'.